Eur. Phys. J. B **49**, 225–230 (2006)
DOI: 10.1140/epjb/e2006-00042-0

THE EUROPEAN PHYSICAL JOURNAL B

Noise induced resonance phenomena in coupled map lattices

G. Ambika[1], K. Menon[1], and K.P. Harikrishnan[2,a]

[1] Department of Physics, Maharaja's College, Cochin-682011, India
[2] Department of Physics, The Cochin College, Cochin-682002, India

Received 12 August 2005 / Received in final form 19 November 2005
Published online 17 February 2006 –

Abstract. We analyse different types of resonance phenomena that can occur in a coupled map lattice in the presence of noise with a subthreshold signal. The onsite dynamics considered here is different from previous such studies, namely, a bimodal cubic map capable of bistability in its dynamics. In addition to the resonance observed in the temporal iterates (the conventional stochastic resonance), we establish the possibility of resonance patterns in spatial sequences along the lattice, which we refer to as "Lattice Stochastic Resonance". The characterising features of both are investigated in detail, under different types of signals with nearest neighbour coupling between lattice points. Possible practical applications are in signal detection, image processing and in communication networks.

PACS. 05.45.Ra Coupled map lattices – 05.40.Ca Noise

1 Introduction

Coupled Map Lattices (CML) are discrete dynamical systems with a spatio-temporal evolution involving large number of degrees of freedom. As such, they are especially useful to model the evolution of collective behaviour in connected systems [1]. They live on a lattice of size N with a prescribed spatial interaction or coupling scheme and a discrete dynamics or map defined at each site. The state of the whole lattice at time t is given by the N-dimensional vector

$$\overline{x}(t) = (x(t,1), x(t,2) \cdots x(t,N))^T \tag{1}$$

The time evolution of this state follows the iterative scheme,

$$\overline{x}(t+1,i) = (I + \tfrac{\epsilon}{2}L)\overline{f}(x(t,i)) \tag{2}$$

where $\overline{f}(x(t,i))$ is the vector governing the local dynamics, I is the identity operator and L is the coupling operator with ϵ as the parameter representing the coupling strength. The most well studied lattice has the diffusive coupling scheme, where $L_{i,i\pm1} = 1$, $L_{ii} = -2$ and $L_{ij} = 0$ otherwise.

Depending on the onsite dynamics, the values of its control parameters and ϵ, the spatio temporal system may evolve into complete synchronisation (CS) [2] i.e., $x(t,i) = x(t)\ \forall i$. Under conditions when CS destabilises, it is capable of other spatial patterns like clusters [3], lattice fractal sets [4], spatio temporal intermittency [5], spatial bifurcations [6] etc. The richness of its dynamics can be enhanced by driving the system with an external signal, which often leads to stable synchronised states, collective periodic behaviour or turbulence [7]. The stability and associated scaling laws in such structures have been recently analysed in detail for different types of onsite dynamics like the logistic map, circle map, Chate-Manneville map etc. [8]. The effect of external noise can also lead to diverse phenomena in this system as discussed by many authors [9]. In general, noise-induced phenomena are found to give better performances in coupled systems or connected arrays than single systems [10] and can be controlled to reach optimum conditions by adjusting the strength of coupling. While small values of spatial coupling lead to spatially blocked configurations or clusters with pinned interfaces, a proper amount of noise helps the system to cross these barriers.

Here we analyse the dynamics of the states formed through a CML by supplying a signal and noise simultaneously to all the lattice points with a local map capable of bistability in its own dynamics. The aim is to keep the signal *subthreshold* and search for possible resonance related phenomena induced by noise. An important phenomenon which can be realised in this respect is the stochastic resonance (SR) [11], with a wide range of practical applications [12,13]. Note that SR in an array of bistable oscillators has been studied previously leading to array enhanced stochastic resonance (AESR) [14] and noise enhanced propagation (NEP) [15]. These results have been extended to CML with various types of onsite dynamics [16]. However, all these studies mainly concentrated on the response of the middle site and its improvement due to spatio temporal synchronisation and spatial connectivity. But our analysis here is different from the previous studies in many ways. Firstly, we employ a

[a] e-mail: kp_hk2002@yahoo.co.in

two parameter, bimodal cubic map for the local dynamics, which has bistability in periodic as well as chaotic attractors [17]. More importantly, since the dynamics of a CML is spatial as well as temporal, we feel that both these aspects should be put into utility for an optimum use of these systems. This is achieved by using spatially recurring static signals and travelling wave trains along the lattice, apart from the usual temporally varying signals at the lattice sites.

The motivation for these studies comes from the following. The CML, being a coupled system, is inherently flexible to handle practical situations through the two additional parameters, *viz*, the system size and strength of coupling. Thus, it is more akin to what natural biological systems do in a self organised way. They use SR to detect weak signals, by adjusting the number of member systems and the strength and nature of coupling among them and try to obtain optimum conditions. This is especially needed for their functioning since the weakness of the signal and quantity and nature of environmental noise vary according to external circumstances beyond their control. There are also other important areas where the above conditions can be applied, such as, for example, signal processing with coupled nonlinear networks (CNN). Moreover, the CML with the bistable cubic map can arise naturally in the study of phase transitions in an actual one dimensional crystal lattice (see Sect. 2) and can also capture the essential features of the evolution process in the study of the nonequilibrium patterns.

We show that SR can occur with all the different types of signals mentioned above. An important novel feature of our work is the introduction of the concept of "Lattice Stochastic Resonance" (LSR), for the detection of spatially varying signals along a CML with the help of background noise. We also discuss some characterising features of LSR, such as, its dependence on, optimum noise amplitude, coupling strength and lattice size.

Our paper is organised as follows. In Section 2, we introduce the type of CML we implement, with the characteristic features of the onsite dynamics chosen. The different types of signals used for the analysis are also introduced. In Section 3, we present the various aspects of SR in the presence of a temporal signal at each lattice site and compare them with the results obtained for AESR. In Section 4, the LSR is introduced and its characteristic features are discussed. The conclusions along with possible future works are given in Section 5.

2 CML as a bistable stochastic resonator

To setup the CML as a stochastic resonator working under bistable mechanism, we choose the onsite map function $f(x)$ as a 2-parameter bimodal cubic map which is a discrete version of the usual double-well potential:

$$f(x(t,i)) = b + ax(t,i) - x(t,i)^3. \tag{3}$$

However, discretisation changes the escape scenario while retaining bistability that can be tuned with greater flexibility using the two parameters a and b involved. Its dynamical possibilities under such variations have been established earlier [17]. For $a = 1.4$, the map has a bistability in one cycle in 'b' window $= [-0.1, 0.1]$ and as a is increased to 2.4, bistability shifts to the chaotic regions through the usual period-doubling scenario. The bistable attractors are clearly separated with $x > 0$ being the basin of one and $x < 0$ that of the other. We have investigated the occurance of SR in a single map of (3) and a system of 2 coupled maps with linear difference coupling [18]. For the present study, we use the same map with $a = 2.4$ and $b = 0.01$ in the regime of bistable chaotic attractors and construct a CML with diffusive, nearest neighbour coupling as

$$x(t+1,i) = (1-\epsilon)f(x(t,i)) + \frac{\epsilon}{2}[f(x(t,i-1)) + f(x(t,i+1))] \tag{4}$$

where t and i refer to the discrete index for time and space and ϵ is the coupling strength for connectivity or diffusive interaction among the maps.

Note that the above model appears in several physical contexts as well. For example, consider a one dimensional crystal lattice with nearest neighbour interaction in the presence of a quartic potential. The standard equation to study phase transitions in such a system is the time dependent Ginzburg-Landau equation for an order parameter field $x(r,t)$ given by

$$\frac{\partial x(r,t)}{\partial t} = Ax(r,t) - Bx(r,t)^3 + C + D\nabla^2 x(r,t) \tag{5}$$

where A, B, C are parameters and D is the diffusion coefficient. Discretising the above equation with nearest neighbour coupling results in (4) [19].

In order to study SR in the system, we add a periodic signal $S(t)$ and a Gaussian random noise $\eta(t)$ of zero mean and a range of variance values from 0.2 to 1 to each lattice site to get

$$x((t+1),i) = (1-\epsilon)f(x(t,i)) + \frac{\epsilon}{2}[f(x(t,i-1)) + f(x(t,i+1))] + ZS(t) + E\eta(t). \tag{6}$$

Here Z and E measure the amplitude of the signal and noise respectively. To exploit the full capacity of the lattice as a resonator, we use four different types of input signals for $S(t)$ as temporal $S_{tp} = \sin(2\pi pt)$, spatial (static) $S_{sp} = \sin(2\pi pi)$, spatio-temporal $S_{st} = \sin(2\pi pit)$ and travelling wave $S_{tw} = \sin(2\pi p(i-t))$. The frequency of the signal in all the cases is fixed at a convenient value, $p = 1/8$.[1] A comparison between the signals is shown in Figure 1, where the variation of each of them along the lattice is plotted at two given time steps $t = 1$ and $t = 5$, for a lattice of size $N = 15$. In the figure, each column represents one type of signal, namely, $(a)S_{tp}$ $(b)S_{sp}$ $(c)S_{st}$ and $(d)S_{tw}$. To analyse the spatio temporal behavior of

[1] The computations have been done for a range of frequencies from 0.1 to 0.3 and we have obtained LSR for all the frequencies.

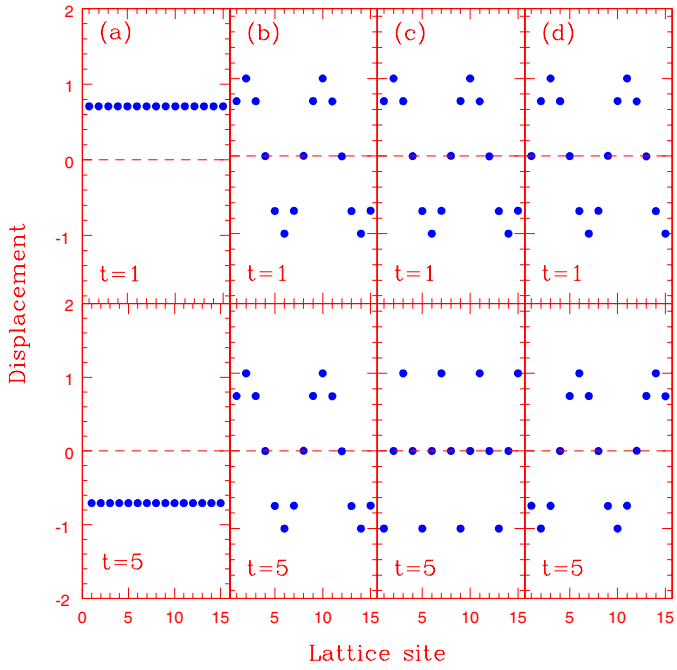

Fig. 1. A comparison between different types of signals used as input to the lattice. Each column represents one type of signal at two different time steps, $t = 1$ (top panel) and $t = 5$ (bottom panel). For the temporal signal S_{tp}, column (a), lattice points are displaced equally from the mean position at a given time step. But each lattice point varies sinusoidally with time. For the other three signals, the displacement consists of a sequence of discrete values with a sine profile which (b) is static in time for the signal S_{sp}, (c) consists of a fundamental and its overtones at different time steps for S_{st} and (d) changes with time for S_{tw}.

the CML under the influence of these signals, the initial conditions of the lattice points are chosen as random and both open and periodic boundary conditions are applied

- open: $x(t,0) = x(t,N+1) = 0$;
- periodic: $x(t,1) = x(t,N+1) \quad \forall t$.

An important criteria for SR is that the signal should be *subthreshold*, that is, its amplitude is sufficiently low so that shuttling between the two basins does not take place without the help of noise. From our previous analysis [18], we have found that this can be achieved if the amplitude of the signal Z is fixed at a value < 0.3 for the signal S_{tp}, where as for the other three signals this is found to be true for $Z < 0.1$.

3 Stochastic resonance with temporal signal

By taking $N = 15$ and S_{tp} as the input signal, the CML is iterated for several thousand time steps with random initial conditions and by tuning the noise amplitude E. The output signal is obtained from the temporal iterates of the middle site ($i = 8$), with a clipping in the window $[-1.5, 1.5]$. It is found that the iterates systematically shuttle between the two basins for an optimum noise amplitude as shown in Figure 2. The temporal behavior of all

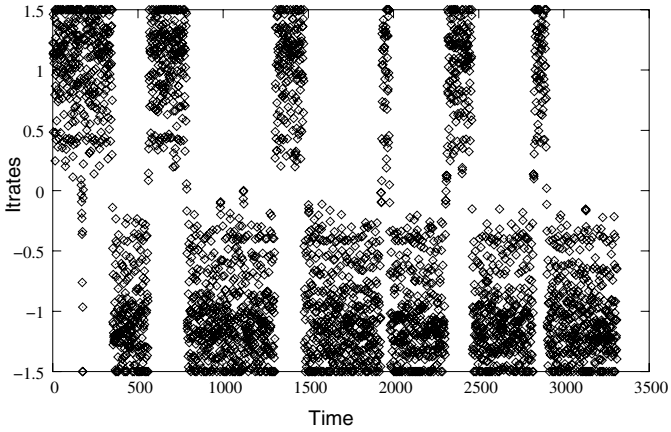

Fig. 2. Time variation of the middle site ($i = 8$) of the CML in the presence of a subthreshold signal S_{tp} with $Z = 0.2$ and noise amplitude $E = 2.185$, indicating SR in the system. The value of the coupling strength $\epsilon = 0.01$.

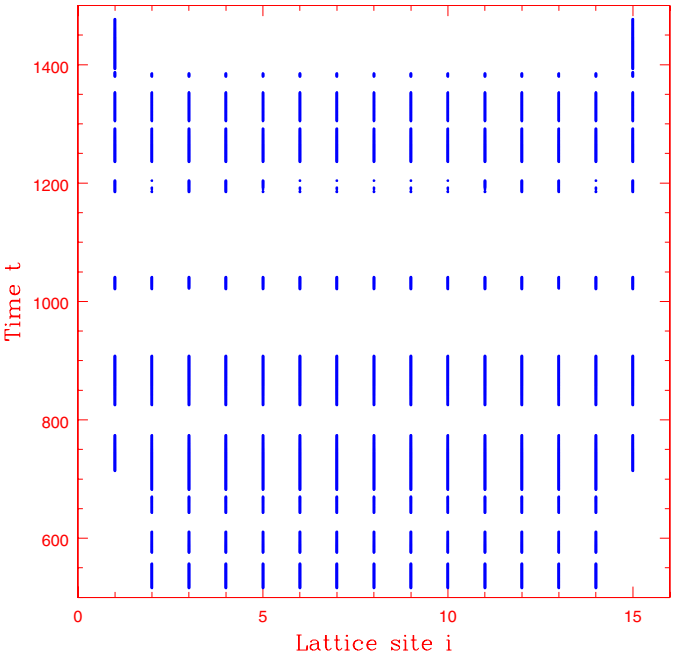

Fig. 3. The space time plot of the CML with the signal S_{tp} and optimum noise amplitude.The first 500 iterates are discarded and the next 1000 iterates are shown for all lattice sites. At each time step, if the lattice site is in the positive basin, it is shown in black. The parameter values are $Z = 0.2$, $E = 2.2$ and $\epsilon = 0.03$.

the lattice sites together is shown in Figure 3 in a space time plot for the optimum noise. It is clear that all the lattice points move in synchronisation with the temporal signal between the two basins.

An important signature for SR is a peak in the output signal to noise ratio (SNR) corresponding to an optimum noise amplitude. To calculate the SNR, the power spectrum of the output is first computed using the FFT algorithm for each value of E. The peak corresponding to the input signal frequency in the power spectrum is taken as S_g and the average value of noise corresponding

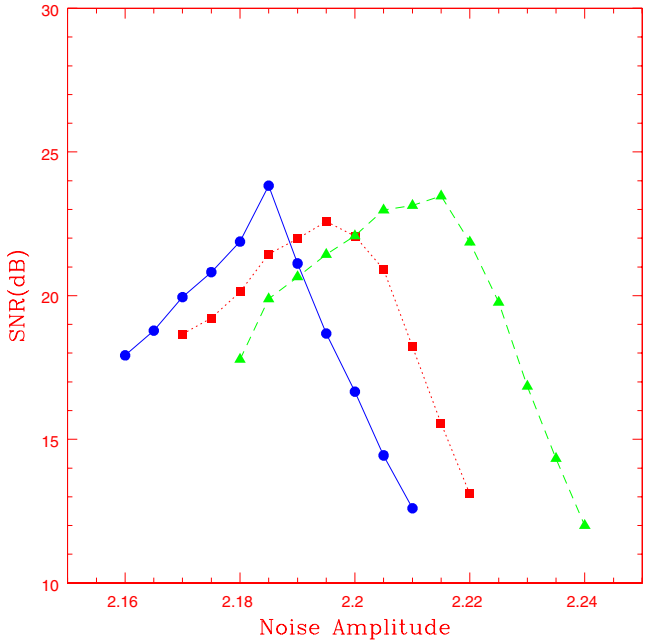

Fig. 4. Variation of SNR with noise amplitude for the middle site ($i = 8$) of the lattice with the signal S_{tp} ($Z = 0.2$) for three values of ϵ, namely, 0.01 (circle connected by solid line), 0.03 (squares connected by dotted line) and 0.05 (triangles connected by dashed line). It is clear that the SNR peak is independent of ϵ, where as, the optimum noise varies approximately linearly with ϵ.

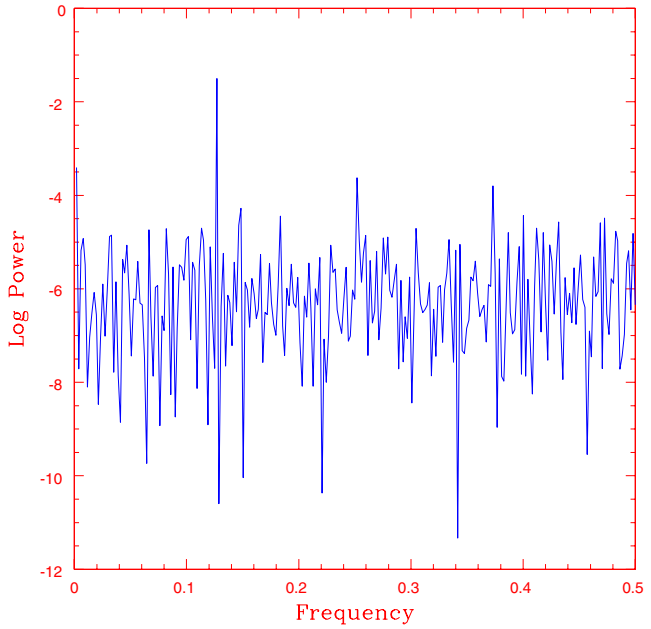

Fig. 5. The power spectrum of the values taken from a frozen pattern along the lattice (of size 512) when a subthreshold spatial signal S_{sp} (with frequency $p = 1/8$ and amplitude $Z = 0.05$) is used as input. The frozen pattern is chosen after discarding initial 10 000 iterations. The peak at the input signal frequency indicates SR spatially along the lattice. Other parameters used are $E = 0.18$ and $\epsilon = 0.002$.

to 10 bins around S_g is taken as noise power N_s. Then the SNR is calculated using the relation

$$SNR = 10 \log_{10} \frac{S_g}{N_s} dB. \tag{7}$$

The whole procedure is repeated for different values of ϵ and the results are shown in Figure 4. A comparison of these results with that obtained for AESR [14] will be interesting at this stage. For the latter, there is an optimum coupling strength at which the response of the chain of oscillators become maximum for a given size of the chain. But in our case, due to the more complex nature of the system and the coupling, the range of ϵ and noise values for the occurance of SR is found to be limited. For very small ϵ, SNR becomes too small and for large ϵ, the signal ceases to be subthreshold and tuning the signal and noise amplitude becomes difficult. For the range of ϵ where the response is optimum, the peak SNR is more or less independent of ϵ, but the optimum noise amplitude shifts towards higher values as ϵ is increased, just as in the case of AESR. Moreover, the response of the middle site improves, in general, with the lattice size for small and moderate values of N (but saturates for large N), indicating a co-operative behavior among the lattice points.

4 Lattice stochastic resonance

We now apply the other three signals discussed above which vary along the lattice and search for SR by tuning various parameters. Two lattice sizes $N = 256$ and $N = 512$ are used in all cases. First, a subthreshold spatial signal S_{sp} is used as the input and the system is iterated using random initial conditions. Note that, here the variation of noise is not just temporal but also spatial as $\eta(t, i)$. That is, at each time step, the noise values are randomly distributed along the lattice. After discarding the initial 10 000 iterations, we choose a "frozen pattern" of all the lattice points along the lattice *at a given time step* as the output signal. We then find that at an optimum noise amplitude, the lattice points are distributed along the lattice in a rhythmic shuttling pattern in tune with the spatial signal. The power spectrum for one such frozen pattern is shown in Figure 5 for a lattice size $N = 512$. The peak corresponding to the input signal frequency $p = 1/8$ is obvious. We have found that any *arbitrary* frozen pattern, after sufficient number of iterations, will behave in an identical manner. In other words, though the lattice points are changing locally in each time step, globally the whole lattice tends to an equilibrium distribution in synchronisation with the subthreshold input signal. It indicates the possibility of a noise assisted detection of the subthreshold spatially varying input signal at the output, much like the conventional SR for a time varying signal at each lattice site.

The whole procedure is repeated using the other two signals as input with similar results. A better way to show the spatio temporal behavior of the lattice is through the space time plot which is shown in Figure 6 for all the three signals for $N = 512$. Note that in all cases, the pattern truly follows the type of input signal used. Also the patterns (a) and (c) for S_{sp} and S_{tw} look similar as expected,

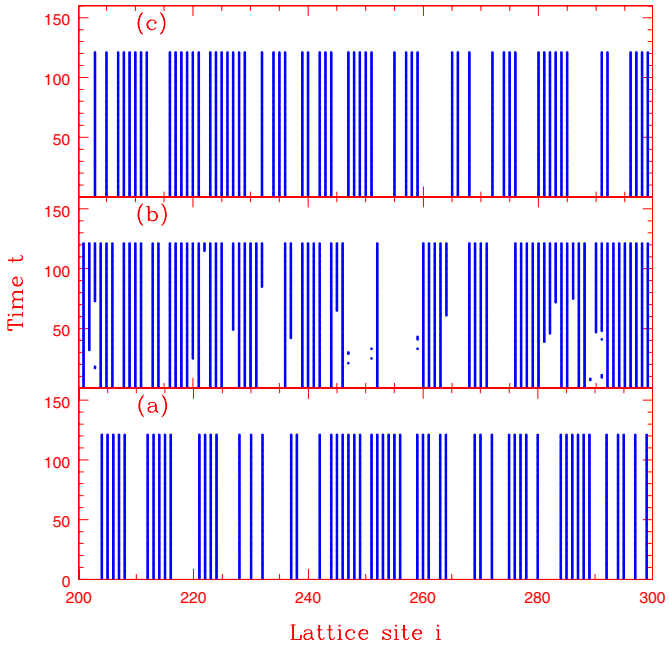

Fig. 6. Space-time plot showing further evidence of SR along the lattice in synchronisation with the signal $(a)S_{sp}$ $(b)S_{st}$ and $(c)S_{tw}$. The noise amplitude is adjusted to be optimum in each case, coupling strength $\epsilon = 0.002$ and lattice size is 512. Here the values for 120 iterates for the middle 100 lattice sites are plotted after discarding initial 10 000 iterations. At each time step, if the value is in the positive basin, it is shown in black.

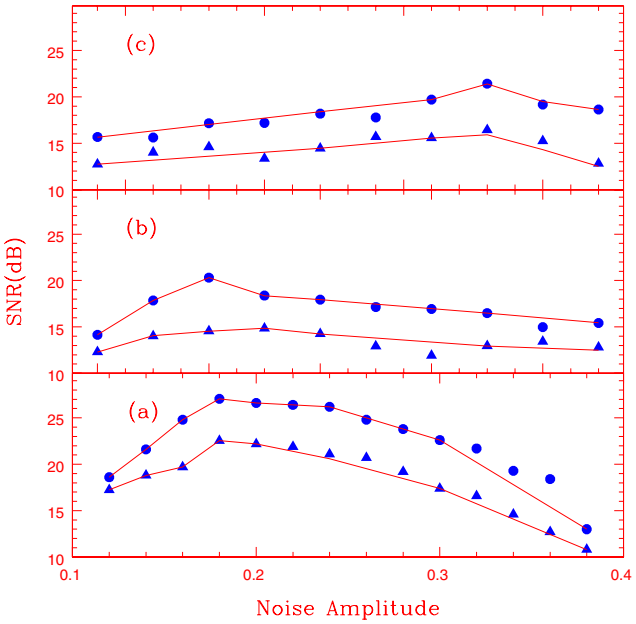

Fig. 7. Variation of SNR with noise amplitude showing LSR for the three input signals $(a)S_{sp}$ $(b)S_{st}$ and $(c)S_{tw}$. Two lattice sizes, 256 (triangles) and 512 (circles), are used in all cases and trend line is shown to aid the eye. Average SNR of a large number of frozen patterns is taken to avoid any spurious effects. The values of Z and ϵ are 0.05 and 0.004 respectively in all cases.

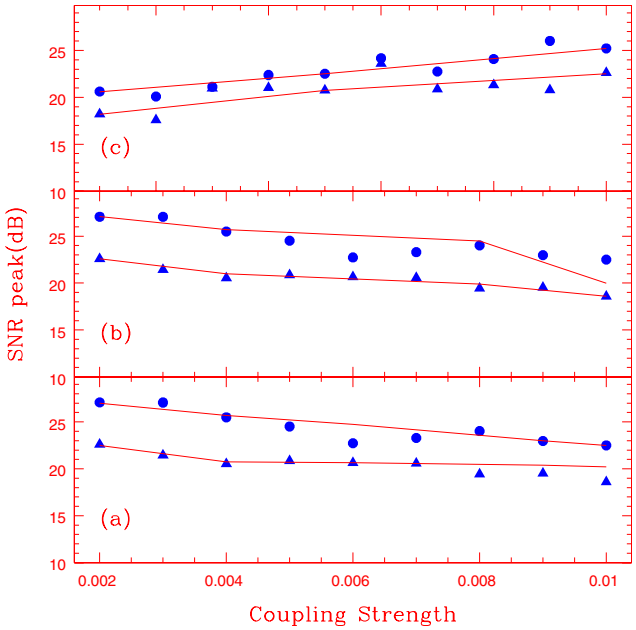

Fig. 8. Variation of SNR peak with ϵ for the three cases of input signals studied in Figure 7 in that order.

but the latter changes with time as the signal travels along the lattice, where as, the former tends towards an equilibrium distribution or pattern in synchronisation with the signal.

Finally, the SNR is calculated from the power spectrum of the frozen pattern for all the cases for a range of values of E. In order to avoid any spurious effects, the calculations are repeated over a number of frozen patterns and the average value of SNR is determined in each case. Its variation with E for two lattice sizes 256 and 512 is shown in Figure 7 for all the signals. Note that due to the effect of averaging, the SNR does not show any strong peaks. But the behavior of the trend lines suggest that, in all cases, there is an optimum noise amplitude (which is different in each case) at which the response of the CML to the input signal is maximum. We call this *Lattice Stochastic Resonance* (LSR) in order to distinguish it from the conventional SR used to detect subthreshold time varying signals from the output SNR. Here also the SNR peak improves with the lattice size, but shows no specific dependence on ϵ as can be seen from Figure 8.

5 Conclusion

Our major motivation in the present work is to bring out the versatile nature of CML as a stochastic resonator and its capacity to handle a variety of signals. We explicitly show that it supports SR both in the temporal and spatial dynamical setups with an onsite dynamics having the minimum required nonlinearity. We use a bimodal cubic map with an inherent escape scenario and bistability window as the onsite dynamics and study SR in the CML using four different types of input signals. We bring out some novel features involving LSR and its dependence on various parameters of CML, such as, the lattice size, and coupling strength. In all the previous studies of SR

involving spatially extended systems, SNR is measured only in the temporal output under spatial or spatio temporal synchronisation or pattern formation. But here we show the possibility of improving the response of a CML in synchronisation with a small subthreshold signal, static or moving along the lattice, with the help of background noise.

This phenomenon may find potential applications in a variety of practical situations. For example, LSR, if extended to information carrying digital signals, can be used beneficially for information coding/decoding in noisy environments. A similar idea has recently been proposed by Morfu et al [20] in what they call a Stochastic Resonator Receiver [SRR] which allows to rescue a subthreshold digital amplitude modulated information signal using a translator of the output of a stochastic resonator. Similarly, if LSR with S_{sp} can be extended to two dimensions, it may be effectively used for signal detection or boosting in image processing with the help of background noise. Noise induced pattern transition and spatio-temporal SR have been realised in practice [21]. Moreover, LSR with S_{tw} and S_{st} can find application with signal transmission in coupled array of communication and neural networks [22]. The LSR can be established further by considering extra setting like one-way coupling,threshold mechanism etc. Such studies are being done and will be reported elsewhere.

G.A. and K.P.H. thank the hospitality and computing facilities in IUCAA, Pune.

References

1. K. Kaneko, *Theory and Application of Coupled Map Lattices* (John Wiley, New York, 1993)
2. W.-W. Lim, Y.-Q. Wang, SIAM-J. Applied Dynamical Systems **1**, 175 (2002); B. Fernandez, P. Guirard, Discrete and Continuous dynamical systems- Series B **4**, 435 (2004); P.G. Lind, J.C. Real, J.A.C. Galles, Phys. Rev. E **69**, 026209 (2004)
3. R. Sridhar, J.A. Glezier, Phys. Rev. Lett. **74**, 3297 (1995); F. Xie, G. Hu, Phys. Rev. E **56**, 1567 (1997); L. Angelini, F. De Carlo, C. Marangi, M. Pellicoro, S. Stramaglia, Phys. Rev. Lett. **85**, 554 (2000); D. Maza, S. Boccaletti, H. Mancini, Int. J. Bif. and Chaos **10**, 829 (2000); I. Belykh, V. Belykh, K. Nevidin, M. Hasler, CHAOS **13**, 165 (2003)
4. G. Ambika, K. Menon, Pramana-J. Phys. **59**, L155 (2001)
5. K. Kaneko, Prog. Theor. Phys. **71**, 1033 (1985); T. Bohr, M. Van Hecke, R. Mikkelson, M. Ipsen, Phys. Rev. Lett. **86**, 5482 (2001)
6. K. Kaneko, Phys. Lett. A **111**, 321 (1985); L.S. Aronson, A.V. Gaponov - Grekhov, M.I. Rabinovich, Physica D **33**, 1 (1988); R.E. Amritkar, P.M. Gade, Phys. Rev. Lett. **70**, 3408 (1993)
7. I. Waller, R. Kapral, Phys. Rev. A **30**, 2047 (1984); S. Jalan, R.E. Amritkar, Phys. Rev. Lett. **90**, 014101 (2003); M. Pineda, M.G. Cosenza, `arXiv:nlin-dyn/ 0504001` (2005)
8. H. Chate, P. Manneville, Phys. Rev. Lett. **58**, 112 (1987); H. Chate, Europhys. Lett. **21**, 419 (1993); W. Wang, Z. Liu, B. Hu, Phys. Rev. Lett. **84**, 2610 (2000); G.R. Pradhan, N. Chatterjee, N. Gupta, Phys. Rev. E **65**, 046227 (2002); M.G. Cosenza, M. Pineda, Parravano, Phys. Rev. E **67**, 066217 (2003); C. Masoller, A.C. Marti, D.H. Zanette, Physica A **325**, 186 (2003); A.C. Marti, C. Masoller, Phys. Rev. E **67**, 056219 (2003); C. Anteneodo, A.M. Batista, R.L. Viana, `arXiv:nlin-dyn/ 0504012` (2005)
9. F. Blondeu, J. Rojas - Varela, Int. J. Bifur and Chaos **10**, 1951 (2000); L. Angelini, M. Pellicoro, S. Stramaglia, Phys. Lett. A **285**, 293 (2001); C. Tao, G. Du, Phys. Lett. A **311**, 158 (2003)
10. M. Locher, D. Cigra, E.R. Hunt, G.A. Johnson, F. Marchesoni, L. Gammaitoni, M.E. Inchiosa, A.R. Bulsara, CHAOS **8**, 604 (1998); I. Rabbiosi, A.J. Scroggie, G. Loppo, Phys. Rev. E **68**, 036602 (2003)
11. L. Gammaitoni, P. Hanggi, P. Jung, F. Marchesoni, Rev. Mod. Phys. **70**, 223 (1998)
12. A. Ganopolski, S. Rahmstorf, Phys. Rev. Lett. **88**, 038501 (2002); G. Balazsi, L.B. Kosh, F.E. Moss, CHAOS **11**, 563 (2001)
13. K.P. Harikrishnan, G. Ambika, Phys. Scripta **71**, 148 (2005)
14. J.F. Lindner, B.K. Meadows, W.L. Ditto, M.E. Inchiosa, A.R. Bulsara, Phys. Rev. Lett. **75**, 3 (1995); J.F. Lindner, B.K. Meadows, W.L. Ditto, M.E. Inchiosa, A.R. Bulsara, Phys. Rev. E **53**, 2081 (1996)
15. J.F. Lindner, S. Chandramouli, A.R. Bulsara, M. Locher, W.L. Ditto, Phys. Rev. Lett. **81**, 5048 (1998)
16. P.M. Gade, R. Rai, H. Singh, Phys. Rev. E **56**, 2518 (1997)
17. G. Ambika, N.V. Sujatha, Pramana-J. Phys. **54**, 751 (2000)
18. G. Ambika, N.V. Sujatha, K.P. Harikrishnan, Pramana-J. Phys. **59**, 539 (2002)
19. R. Kapral, M.N. Chee, G. Whittington, *Measures of Complexity and Chaos*, Ed. N.B. Abraham et al. (Plenum Press, New York, 1994)
20. S. Morfu, J.M. Bilbault, J.C. compte, Int. J. Bif. and Chaos **13**, 233 (2003)
21. H. Zhonghuai, Y. Lingfa, X. Zuo, X. Houwen, Phys. Rev. Lett. **81**, 2854 (1998)
22. H.E. Plasser, T. Geisel, Phys. Rev. E **63**, 031916 (2001)